SWIFT XRT CALDB RELEASE NOTE

SWIFT-XRT-CALDB-09:

Position-Dependant Windowed Timing Response Matrices

Table P1: Files released

Filename	WT Grade	Substrate† voltage (V)	Detector‡ Position	Start Date	End Date
swxwt0to2s0psf1_20010101v001.rmf swxwt0s0psf1_20010101v001.rmf	0 − 2 0	0	1	2001-Jan-01	2006-Dec-31
swxwt0to2s0psf2_20010101v001.rmf swxwt0s0psf2_20010101v001.rmf	0 − 2 0	0	2	2001-Jan-01	2006-Dec-31
swxwt0to2s0psf3_20010101v001.rmf swxwt0s0psf3_20010101v001.rmf	0 − 2 0	0	3	2001-Jan-01	2006-Dec-31
swxwt0to2s0psf1_20070101v001.rmf swxwt0s0psf1_20070101v001.rmf	0 − 2 0	0	1	2007-Jan-01	2007-Aug-30
swxwt0to2s0psf2_20070101v001.rmf swxwt0s0psf2_20070101v001.rmf	0 − 2 0	0	2	2007-Jan-01	2007-Aug-30
swxwt0to2s0psf3_20070101v001.rmf swxwt0s0psf3_20070101v001.rmf	0 − 2 0	0	3	2007-Jan-01	2007-Aug-30
swxwt0to2s6psf1_20070901v001.rmf swxwt0s6psf1_20070901v001.rmf	0 − 2 0	6	1	2007-Sep-01	2008-Dec-31
swxwt0to2s6psf2_20070901v001.rmf swxwt0s6psf2_20070901v001.rmf	0 − 2 0	6	2	2007-Sep-01	2008-Dec-31
swxwt0to2s6psf3_20070901v001.rmf swxwt0s6psf3_20070901v001.rmf	0 − 2 0	6	3	2007-Sep-01	2008-Dec-31
swxwt0to2s6psf1_20090101v001.rmf swxwt0s6psf1_20090101v001.rmf	0 − 2 0	6	1	2009-Jan-01	2010-Dec-31
swxwt0to2s6psf2_20090101v001.rmf swxwt0s6psf2_20090101v001.rmf	0 − 2 0	6	2	2009-Jan-01	2010-Dec-31
swxwt0to2s6psf3_20090101v001.rmf swxwt0s6psf3_20090101v001.rmf	0 − 2 0	6	3	2009-Jan-01	2010-Dec-31
swxwt0to2s6psf1_20110101v001.rmf swxwt0s6psf1_20110101v001.rmf	0 − 2 0	6	1	2011-Jan-01	2012-Dec-31
swxwt0to2s6psf2_20110101v001.rmf swxwt0s6psf2_20110101v001.rmf	0 − 2 0	6	2	2011-Jan-01	2012-Dec-31
swxwt0to2s6psf3_20110101v001.rmf swxwt0s6psf3_20110101v001.rmf	0 − 2 0	6	3	2011-Jan-01	2012-Dec-31
swxwt0to2s6psf1_20130101v001.rmf swxwt0s6psf1_20130101v001.rmf	0 − 2 0	6	1	2013-Jan-01	2013-Dec-11
swxwt0to2s6psf2_20130101v001.rmf swxwt0s6psf2_20130101v001.rmf	0 − 2 0	6	2	2013-Jan-01	2013-Dec-11
swxwt0to2s6psf3_20130101v001.rmf swxwt0s6psf3_20130101v001.rmf	0 − 2 0	6	3	2013-Jan-01	2013-Dec-11
swxwt0to2s6psf1_20131212v001.rmf swxwt0s6psf1_20131212v001.rmf	0 − 2 0	6	1	2013-Dec-12	—
swxwt0to2s6psf2_20131212v001.rmf swxwt0s6psf2_20131212v001.rmf	0 − 2 0	6	2	2013-Dec-12	—
swxwt0to2s6psf3_20131212v001.rmf swxwt0s6psf3_20131212v001.rmf	0 − 2 0	6	3	2013-Dec-12	—

† The substrate voltage was permanently raised from $V_{ss} = 0\,\mathrm{V}$ to $V_{ss} = 6\,\mathrm{V}$ on 2007-Aug-30.

‡ psf1: $DETY = 300.5 \pm 10n$, psf2: $DETY = 303.0 \pm 5n$, psf3: $DETY = 305.5 \pm 10n$, (with $n = 0, 1, 2 \ldots$)

Scope of Document

This document describes the release of *Swift*-XRT Windowed Timing (WT) position-dependant redistribution matrix files (RMFs), calculated assuming a point-source illumination model at three locations with respect to the WT readout 10-row binning boundary. These files supplement those previously released assuming a uniform source illumination model, which were previously thought to be generally applicable for point-like or extended sources. The new files have slightly different low-energy redistribution properties, which can be evident when fitting WT spectra from moderate to heavily absorbed sources.

Introduction

One of the principle modes of operation of the *Swift*-XRT is Windowed Timing (WT) mode (e.g. Hill et al., 2005, SPIE, 5898, 313), whereby the CCD is continuously clocked in the parallel direction, until 10 rows have accumulated in the serial register, at which point the central 200 pixels of the latter are read out and the process repeats. WT mode is selected automatically by the XRT for bright sources (typically $> 2-10 \, \mathrm{count \, s^{-1}}$ [i.e. $2.5-12.8$ milliCrab], depending on whether the XRT is leaving or entering WT mode) in order to limit pile-up, or can be requested for Target of Opportunity (TOO), Guest Investigator (GI) or fill-in observations if the proposer wishes to utilize the higher time resolution (1.77ms) that the mode provides.

In WT mode, large, multipixel events that fall across a 10-row binning boundary are split into two events of lower energy by the WT readout scheme and contribute to the strong redistribution tail (in grade 0) and a $0.5-1 \, \mathrm{keV}$ 'bump' (in grades 1–2) seen in WT observations of absorbed sources.

The default WT mode RMFs (described in release notes SWIFT-XRT-CALDB-09_v17, SWIFT-XRT-CALDB-09_v18 and SWIFT-XRT-CALDB-09_v19) were calculated using a uniform intensity distribution for the source of incident X-rays illuminating the CCD. However, simulations using the XRT point source (PSF) model to describe the spatial distribution of incident photons reveal that the strength of the WT redistribution tail changes slightly compared with the uniform source case. Furthermore, the effect is dependent on the location of the centre of the source PSF with respect to the 10-row binning boundaries. This occurs because a higher fraction of incoming photons are concentrated at the centre of the PSF, so more events are available for splitting when the source centre is positioned on a 10-row binning boundary compared with the case when the source's centre is offset by, for example, 5 pixels.

Additionally, the strength of the redistribution tail is found to be dependent on the value of the event threshold used to calculate the RMF. The WT event threshold was set to 80 DN onboard shortly after launch. However, the gradual increase of the CCD Charge Transfer Inefficiency (CTI) and the evolution in the distribution of deep charge traps means that in real energy terms, the threshold has increased slowly with time. For example, in 2005-January the threshold occurred at $210 \, \mathrm{eV}$ whereas in 2013-November it was close to $\sim 320 \, \mathrm{eV}$. To counter this increase, the XRT team lowered the onboard WT threshold to 60DN ($\sim 260 \, \mathrm{eV}$) on 2013-December-11.

Figure 1 shows example model spectra illustrating both the position dependence (top row) and threshold dependence (bottom row) of the WT RMFs.

Position-Dependant WT RMFs

Given the findings above, we have calculated a number of point source position- and epoch-dependant WT RMFs which are listed in table P1. The RMFs were computed using the same broadening and event thresholds employed to create the uniform source epoch dependent RMFs (see SWIFT-XRT-CALDB-09_v19 and references therein), with table 1 showing the inputs used by the MC simulation code which generates the RMF.

The new position-dependant RMFs are distinguished from the uniform illuminated case RMFs by the inclusion of the characters 'psf' in their file names, as follows :

swxwt*G*s*S*psf*P*_*YYYYMMDD*v001.rmf

where G is the grade selection (either '0' or '0to2'), S is the substrate voltage (either '0' for pre- 2007/08/31 observations, or '6' thereafter), P is the CCD DETY position number that the RMF was calculated at (either '1',
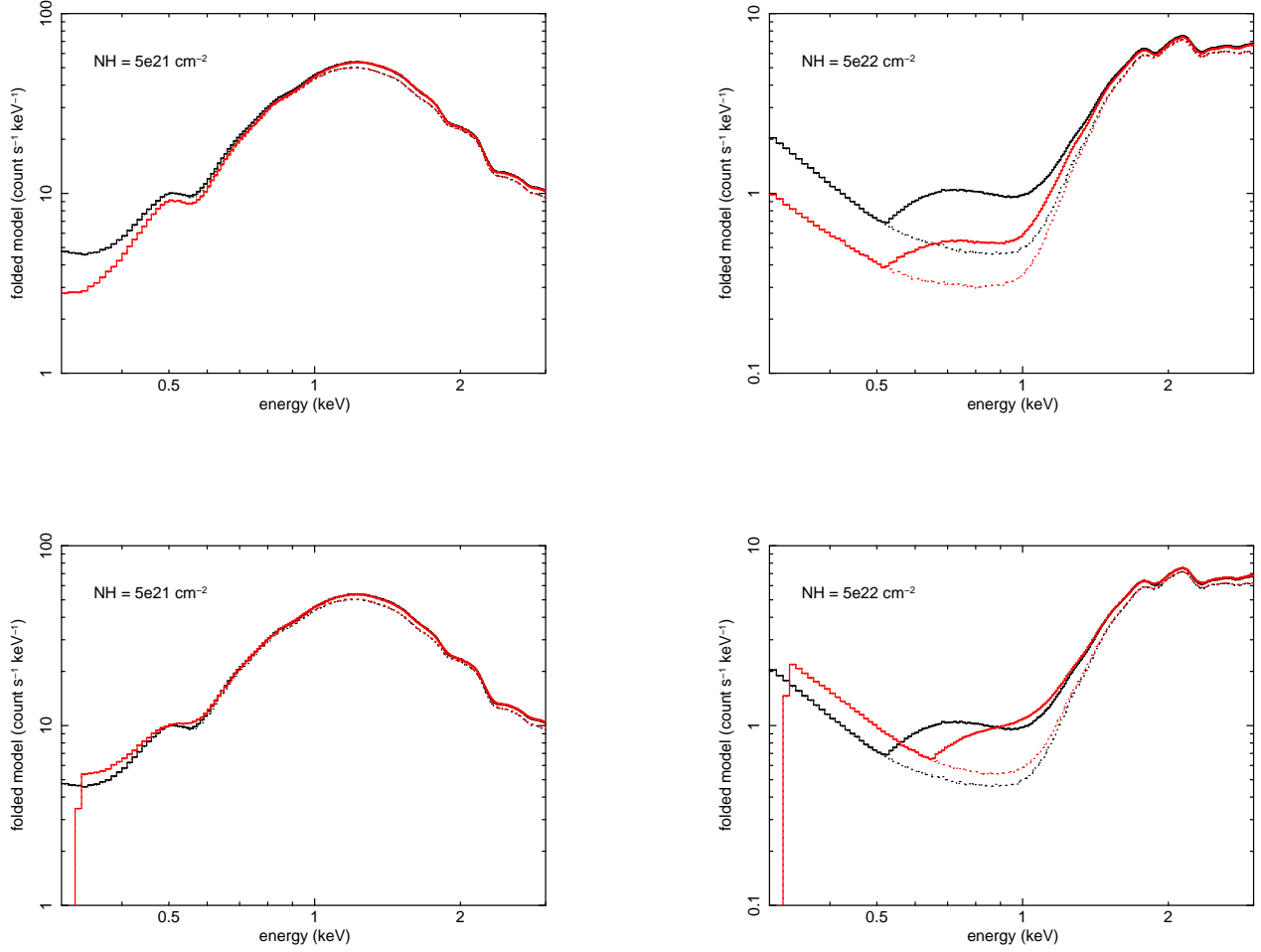
Figure 1: WT simulations of a point source, assuming a $\Gamma = 2$ powerlaw incident spectrum absorbed by 5×10^{21} atoms cm^{-2}, on the left, and 5×10^{22} atoms cm^{-2}, on the right. The top row compares spectra obtained at different locations on the CCD, with the black spectra appropriate for a source located on a WT 10-row binning boundary (in this case at DETY=300.5), while the red spectra are for a source positioned 5 pixels away from the 10-row binning boundary (DETY=305.5). The bottom row compares spectra obtained for different event thresholds of 250 eV (black) and 320 eV (red) (computed at DETY=300.5). For both rows, solid curves show grade $0 - 2$ and dotted curves grade 0. (Note, the grade 0 and grade $0 - 2$ spectra are almost identical in the left panels.)

Table 1: CCD Monte-Carlo simulator inputs and RMF minimum usable energy.

Epoch	EN $(e^-)^\star$	CTI$_s$†	CTI$_p$‡	Threshold (eV)$^\diamond$	Minimum E (keV)$^\spadesuit$
				WT	WT
2007-Sep-01	7.5	3.5×10^{-5}	3.5×10^{-5}	220	0.30
2009-Jan-01	8.5	5.0×10^{-5}	5.0×10^{-5}	255	0.33
2011-Jan-01	9.0	6.0×10^{-5}	6.0×10^{-5}	270	0.35
2013-Jan-01	9.5	6.0×10^{-5}	1.0×10^{-4}	290	0.40
2013-Dec-12	9.5	6.0×10^{-5}	1.0×10^{-4}	270	0.30

* electronic noise (σ); † serial CTI; ‡ parallel CTI; $^\diamond$ MC input threshold — NB the effective threshold is $\sim (1 - CTI_s)^{-300}(1 - CTI_p)^{-900} \times$ higher; $^\spadesuit$ approximate lowest usable energy when fitting
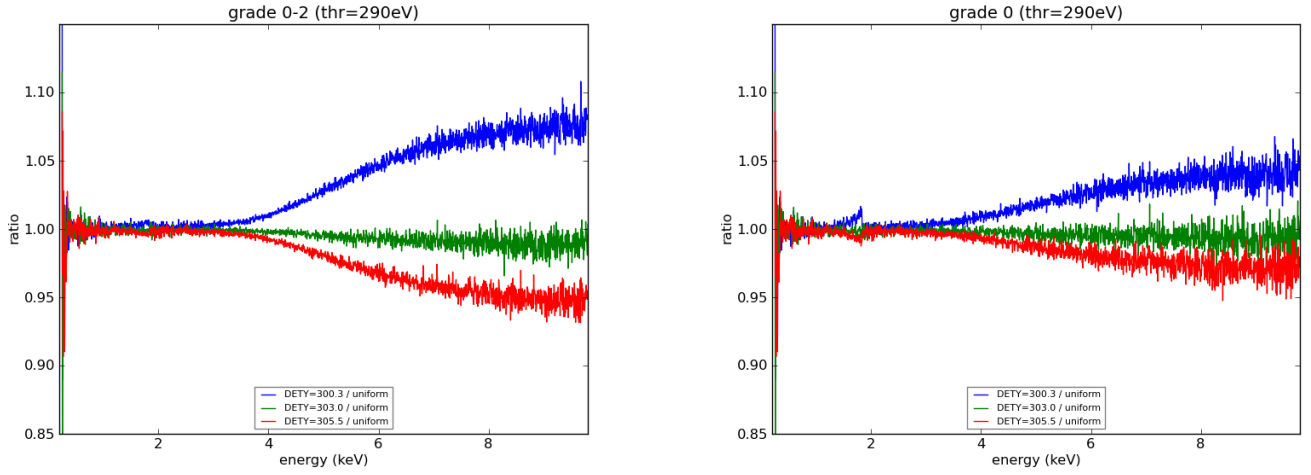
Figure 2: Ratio of the QEs seen from the position-dependant RMFs compared with the uniform source RMF for grade $0 - 2$ (left) and grade 0 (right).

'2', or '3', see below) and $YYYYMMDD$ is the epoch the RMF should be used from. The RMFs have the version number 001 as these are the first release of the position-dependant RMFs.

The RMFs were computed with the centre of the source PSF at the following detector positions :

RMF	DETY	Comment
psf1	$300.5 \pm 10n$	Maximum amount of 10-row binning induced event splitting (i.e. strongest redistribution).
psf2	$303.0 \pm 5n$	Average amount of 10-row binning induced event splitting. (Comparable to uniform source RMF.)
psf3	$305.5 \pm 10n$	Minimum amount of 10-row binning induced event splitting (i.e. weakest redistribution).

(with n equal to 0, 1, 2 . . .). Note, because of the symmetry imposed by the 10-row binning readout scheme, a source located at DETY of 303.0 is equivalent to one at 298.0 or 308.0, etc.

Figure 2 compares the ratio of the quantum effiency (QE) from the position-dependant RMFs to the QE from the uniform source RMF and illustrates that there are small QE changes associated with the choice of RMF (and hence on the measured spectral parameters — for example, 0.04 in photon index for a typical $\Gamma = 2$ powerlaw model), caused by the effects of grade migration.

In WT mode, the DETY position of an event is reconstructed by the task *xrttimetag*, using such information as the input source position (i.e. its RA and Dec) and the spacecraft attitude. Unfortunately, at this point in time, the latter is not known well enough to predict the DETY location of the source with sufficient accuracy at the pixel level in order to choose the appropriate position-dependant RMF to use[1]. Instead, we envisage users who think their WT observations might be affected by 10-row binning induced redistribution issues (see 'Applicability', below) will use these RMFs to explore any possible systematic effects when spectral fitting. To first order, this can be achieved by essentially treating the RMF as an additional fitting parameter and repeating the analysis using the three positional RMFs in turn, then, for simple models, the RMF which returns the lowest fit statistic will be the most likely one to use for the spectrum being analysed.

Figures 3 and 4 show example spectra where using the position-dependant RMFs improve the fit to the low energy redistribution residuals compared with the uniform source RMF.

---

[1]It's possible that, in the future, improved attitude files will be made available for use in XRT analysis, which should provide a more accurate detector position reconstruction than the currently available 'sat' or 'pat' files.
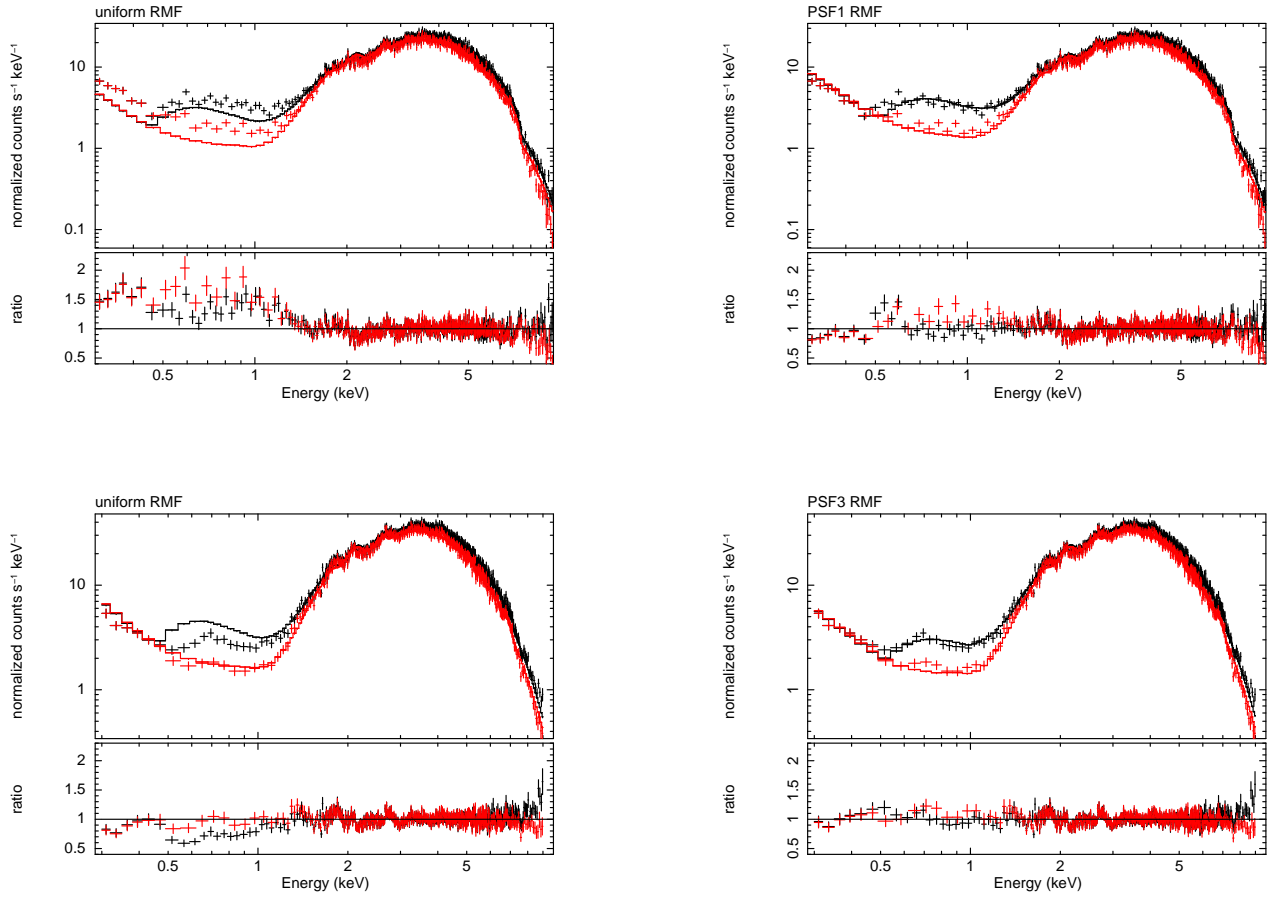
Figure 3: HMXRB Cygnus X-3 WT spectra (grade 0 − 2 in black, grade 0 in red) from two consecutive snapshots taken on 2008-Apr-26. The top left panel shows the first snapshot of data fit using the RMF generated for an uniform intensity distribution created for this epoch. The top right panel shows the same data fit with the psf1 RMF for this epoch. The bottom left panel shows the second snapshot of data fit using the uniform source RMF. The bottom right panel shows the second snapshot fit with the psf3 RMF. In both cases, the position-dependant RMFs fit the low energy redistribution better in this heavily absorbed source.
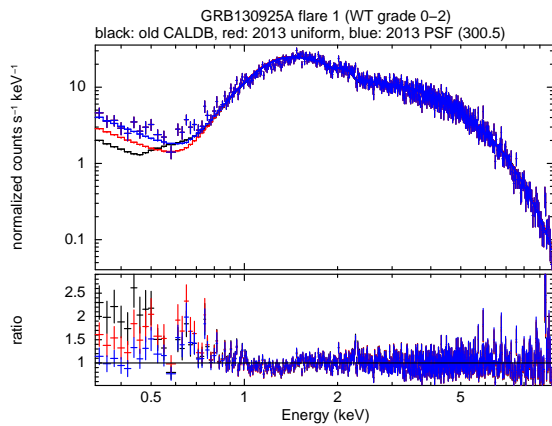

Figure 4: GRB130925A grade 0 − 2 spectrum (obtained during the first flare interval) modelled with the 20070901 uniform source RMF (black), the 20130101 uniform source RMF (red) and the 20130101 psf1 RMF (blue). The latter RMF models the low energy redistribution tail most effectively.

Applicability

It is expected the files released here will be useful when fitting WT spectra obtained during single snapshots from moderate to heavily absorbed sources (NH $> a\ few \times 10^{21}\,\mathrm{cm}^{-2}$), especially if the spectra show departures from the model at low energies (below $\sim 0.5 - 1\,\mathrm{keV}$, depending on the level of absorption) when the default, uniform source, RMFs are used.

The files will be less useful for spectra which are summed over multiple snapshots, as this averages out the position-dependant effects reported here. Likewise, the impact of any position-dependant effects will be reduced when a source is piled-up and the core of the PSF has been excised, or if the source centre falls on the CCD bad-column gap, as the fraction of events falling at a given pixel location will no longer be biased towards the core of the PSF and will be more consistent with the uniform-source generated RMFs.

Note, while the epoch dependent files were generated with a certain range of dates in mind, our choice of date boundaries in making these RMFs reflects the continuous evolution of the CCD response, and does not relate to any quantised performance changes at these precise dates. Hence, if a source is observed either just before (or after) a given RMF starting date epoch (from table P1) then it is possible the RMFs from the following (or preceding) epoch will work equally as well (as the effects caused by changing the threshold is of secondary importance compared with the position dependence).

Table 1 includes an estimate of the epoch dependant minimum energy to use when spectral fitting. The values, obtained by averaging data over multiple snapshots, are somewhat approximate, as the minimum energy depends on the effective threshold, which in turn depends on trap depths and locations, and can vary with the position of the source on the detector. Hence, it is possible that a specific snapshot of data could have a minimum usable energy higher (or lower) than those listed here.

Useful Links

Summary of XRT RMF/ARF releases	http://www.swift.ac.uk/analysis/Gain_RMF_releases.html
XRT analysis threads at the UKSSDC, University of Leicester	http://www.swift.ac.uk/analysis/xrt/
XRT digest pages at the UKSSDC, University of Leicester	http://www.swift.ac.uk/analysis/xrt/digest.php
IACHEC website	http://web.mit.edu/iachec/